Extended G-Band Planar Frequency Tripler for Broadband Instrumentation

Tom Roberts, Jon Martens

[Summary] To extend the frequency range of broadband microwave and millimeter-wave test equipment, broadband frequency sources are required. The design and development of a zero-bias, extended G-Band (130 GHz to 260 GHz) planar frequency Tripler is presented. This Tripler design uses discrete, Schottky barrier diode (SBD) Varistors. The design is inherently balanced and provides excellent unwanted harmonic suppression. The effects of package parasitics, via inductance and unbalance effects on diode parameters are examined. At an input drive level of +10 to +15 dBm, the multiplier delivers an output power level of −6 to 0 dBm from 130 GHz to 240 GHz.

1 Introduction

Miniature commercial NLTL-based reflectometers were recently introduced[1) to 3)], and were shown by their authors to extend the frequency range of a microwave VNA to 110 GHz, and shortly thereafter to 145 GHz. In their approach[1) to 3)], the VNA receivers were extended from 30 GHz to 110/145 GHz by means of monolithic NLTL samplers[4)], broadband high-directivity directional couplers, and a 1.0/0.8-mm coaxial-port connector. These NLTL-based reflectometers require source signals that extend to the system frequency limit. Typically, these source signals are multiplexed onto the main-line to form an ultra-wideband source at the instruments test port. A portion of the source signal is coupled to the reference channel. The rest of the signal is reflected from the DUT and transmitted through the DUT arriving at their respective test channels. For the case of active device characterization, low spurious and unwanted harmonic content of the source signal is important since the DUT's characteristics may change with the presence of these signals.

NLTL Distributed Harmonic Generators (DHG) can used to extend the CW source from 54 GHz to 110/145 GHz. However, their required input drive level must be approximately +24 dBm to minimize conversion loss (and maximize output power) of the wanted harmonic output tone. Amplifiers that have P1dB = +24 dBm in the range of 45 GHz to 75 GHz to drive a DHG do not exist. In addition, unwanted harmonics must be filtered at the DHG's output. To overcome these challenges, a multiplier with lower required input drive power, broadband operation and a balanced structure to naturally suppress the second harmonic is needed. The difficulty in meeting the input drive and unwanted harmonic suppression requirements of the DHG provided motivation to find a new multiplier solution that can provide a source signal over the extended G-Band.

Wideband planar D and Y band Frequency Triplers have been design, developed and discussed[5)]. Variations on the design have been explored but simulation results of conversion loss or efficiency did not agree well with measurements over their entire waveguide bands. Other Waveguide-band triplers have been developed[6)]. Although these have exceptional output power and efficiency, only a portion of the waveguide band is covered.

This article reports the design, development and evaluation of an extended G-Band planar frequency Tripler. The block diagram of the planar Tripler is first described including a test plan. A description of the design of each block is provided with 3D Electromagnetic (EM) simulation results. Design considerations such as diode and substrate selection are discussed. The 3D model of each diode is included in the Electromagnetic simulation to account for diode package parasitics. For each diode, internal EM ports are used in the 3D EM model to co-simulate the diodes SPICE junction parameters in a Harmonic Balance Simulator. Finally, measurement results are presented comparing the simulated vs. measured performance. The end goal of this project was not to necessarily construct a stand-alone G-Band Tripler module as an end product, but to evaluate the suitability of the Planar Tripler element which could be integrated into a multi-functional millimeter-wave module.

2 G-Band Tripler Block Diagram

Shown in Figure 1 is a block diagram of the Extended G-Band Tripler. The Tripler uses two commercially available discrete Schottky anti-parallel Varistor diodes on either side of the main line. An 80 GHz Stepped Impedance Resonator (SIR) Low Pass Filter (LPF) reflects harmonics of the input signal and prevents all generated harmonics originating from the anti-parallel diode pairs from being absorbed back into the input. A 130 GHz Substrate Integrated Waveguide (SIW) High-pass filter (HPF) passes the ×3 harmonic, reflects the fundamental and partially reflects the unbalanced ×2 harmonic. It is expected the ×5 harmonic is at least 10 dBc down from the third harmonic aided by losses at the output.

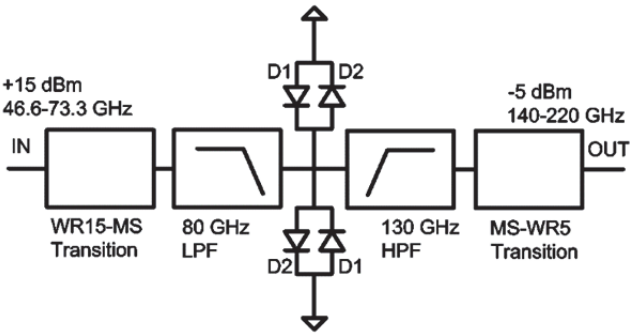

Figure 1 Block diagram of the Extended G-Band Tripler.

To facilitate testing, low-loss longitudinal E-Plane Microstrip-to-Waveguide transitions were used to transition to standard WR15 and WR5 waveguide test interfaces. The input filter, output filter, anti-parallel diode pairs and WR15-Microstrip (MS) transition probe are all integrated onto one planar 4-mil thick Fused Silica substrate. The MS-WR5 transition probe substrate was designed as a 4-mil thick Fused Silica substrate with a reduced substrate width.

3 A Case For Two Anti-Parallel Diode Pairs

The harmonic content of an ideal square wave has only odd harmonics and the aim of this design is to drive the two anti-parallel diode pairs so that clipping occurs at both the maximum and minimum drive signal levels. The 2nd and 4th harmonic idler impedances are short circuits as the diode currents at these frequencies circulate within the loop of the diodes[7]. Ideal short circuits may not exist if diodes or parasitics are mismatched. Figure 2 shows the diode states at the positive input voltage extreme with diode package capacitance assumed negligible. D2 of the upper diode pair (See Figure 1) is forward biased and its equivalent series resistance Rs2 of 10Ω is shown. Diode D1 of the upper diode pair is reversed biased and looks like a high impedance with its junction capacitance of approximately 2.5 fF. Lvia is the inductance of the 125 micron diameter metalized via on the Fused Quartz substrate. For the lower diode pair, the same conditions apply for D2 and D1 respectively at the positive input voltage extreme. For the negative input voltage extreme, the roles of anti-parallel diodes D1 and D2 alternate with one another.

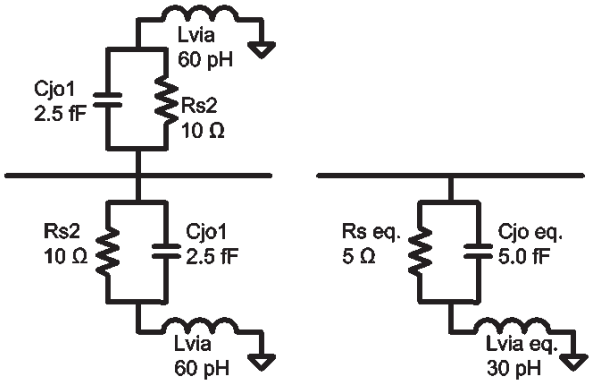

Figure 2 Lumped models of Anti-parallel diodes at positive input voltage extreme and their equivalent impedances.

At 220 GHz, the impedance of the reversed bias diodes is 241Ω and the impedance of each via is 83Ω. Relative to the 10Ω series resistance of the forward biased diodes, the reversed-bias diode impedance is large and appears open. With respect to the impedance seen on the main line, these two networks are in parallel and the impedance is halved as shown in Figure 2. A low impedance path for the forward-biased diodes is desirable from the standpoint of conversion efficiency and bandwidth. Further, the two anti-parallel diode pair arrangement allows for increased power handling. On the other hand, if each diode pairs' junction parameters are not matched then the two diode pairs will produce imbalances and worsen the 2nd and 4th harmonic response.

The inductance of the Fused Quartz 125 μm diameter via was found using Sonnet Software[8] by de-embedding the measurement ports to the diode attachment point. The forward-biased diode was modeled as an ideal 10Ω element connecting to a 125 μm diameter via. See Figure 3. This structure was simulated with and without symmetry applied to obtain the results of the single and parallel resistor and via arrangement. The 2-port EM simulation models

(.s2p) were fitted against a series RL lumped element network (in shunt) to extract the value of Lvia and verify the equivalent values of Rs_eq. and Lvia_eq.

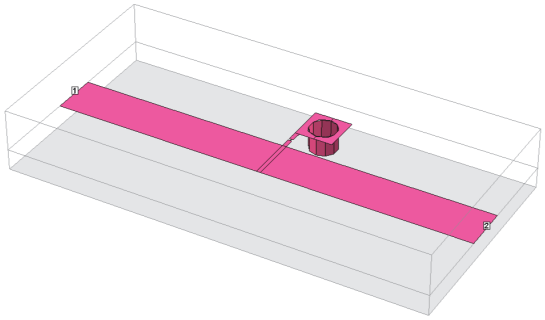

Figure 3 Sonnet model of 125 µm diameter via on 100 µm Fused Quartz.

4 Input and Output Harmonic Filters

As shown in Figure 4, an 11-order Stepped Impedance Resonator (SIR) LPF was designed on 4-mil thick Fused Silica and simulated in CST Microwave Studio[9] to filter harmonics from the source input and reflect harmonics generated originating from the Anti-parallel diode pairs. A minimum line width of 25 µm sets the high-impedance sections to 125Ω. A maximum line width of 515 µm sets the filters minimum impedance at 27Ω. The high impedance line is large enough so techniques like Defected Ground Structures (DGS) do not need to be used to further increase their impedance. Simulation results of this filter (Figure 4) show better than 40 dB stopband rejection from 110 GHz to 220 GHz. Figure 5 shows a plot of the complex impedances of the fundamental, 2nd and 3rd harmonics looking back into the LPF from the diodes mainline attachment point.

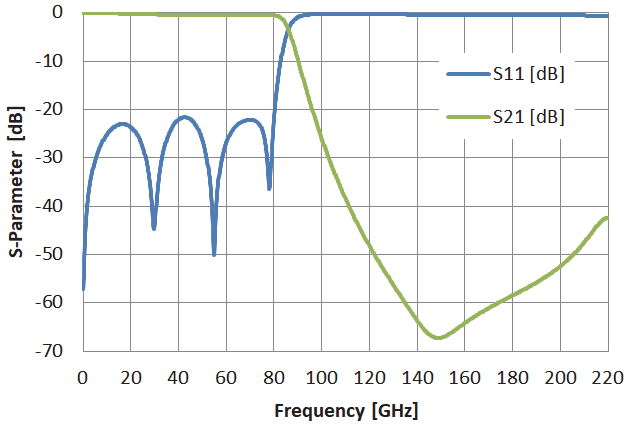

Figure 4 80 GHz 11th Order SIR LPF frequency response.

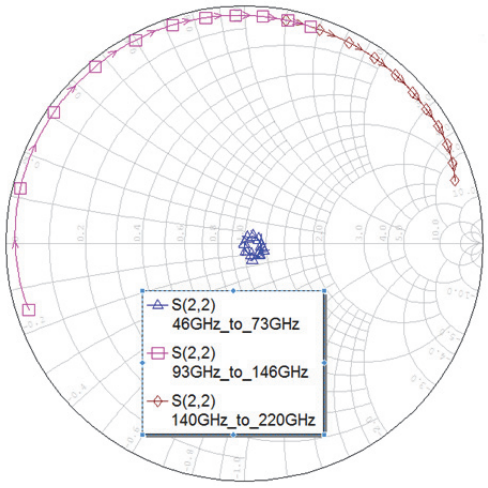

Figure 5 Complex harmonic impedances from diode mainline attachment point looking back into the 80 GHz 11th Order SIR LPF.

The output Substrate Integrated Waveguide (SIW) HPF shown in Figure 6 has a corner frequency of 130 GHz. The primary role of this filter is to suppress the fundamental input signal and partially suppress the ×2 harmonic. Since the HPF corner frequency is 130 GHz, the second harmonic is only attenuated over the lower frequencies from 93 GHz to 130 GHz. Reliance on good diode balance is critical to suppress generation of the second harmonic. To improve the filter's return loss, the input and output transmission lines include radii[10), 11)] and the outer ground vias at the filters interior are moved slightly inward. The walls of the waveguide are provided by the outer ground vias. Each via has diameter of 125 µm with center-to-center spacing of 250 µm. The mean lateral center-to-center distance between the outer ground vias is 713 µm which sets the waveguide cutoff frequency at 130 GHz. Figure 7 shows the complex impedances of the fundamental, 2nd and 3rd harmonics. The 2nd harmonic is only partially reflected by the output HPF.

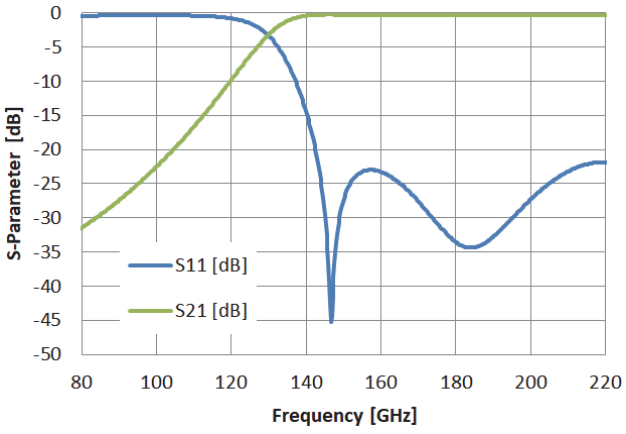

Figure 6 130 GHz SIW HPF frequency response.

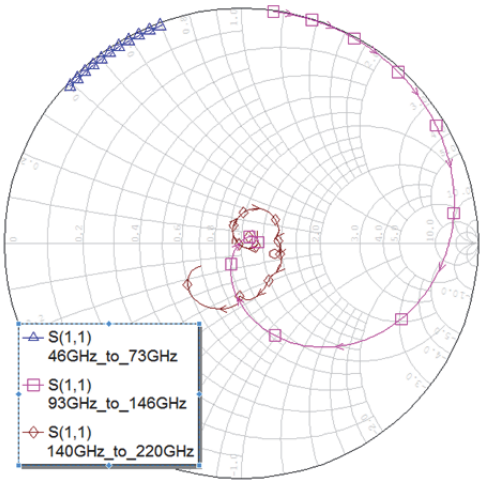

Figure 7 Complex harmonic impedances from diode mainline attachment point looking forward into the 130 GHz SIW HPF.

5 Modeling the Anti-Parallel Diodes

Diode package parasitics such as package capacitance can play a role in determining the diodes bandwidth and usability up to the maximum frequency of operation. Diode vendors have reduced the height and overall package size to reduce package capacitance. The diode's package was modeled using the diodes base substrate material, metal geometry, and diode junction locations. Internal ports were placed at the junction of each anti-parallel diode as shown in Figure 8. Incorporating the diodes package model and junction locations into the 3D model separates the package characteristics from the SPICE parameters of the diodes junction model. The diode's junctions are small compared to the minimum wavelength by the equation

$$\lambda_{min} = c_0/(\sqrt{\varepsilon_{eff}} * f_{max}) \quad (1)$$

and allows lumped port modeling of the diode junctions within the 3D EM simulator. The final 3D simulation results of the composite six port model (four internal ports for each diode and two waveguide ports) including filters, diode packages and Waveguide-to-Microstrip transitions were then exported to an .s6p file. This composite model takes into account all strong near-field interactions between sub-circuit elements.

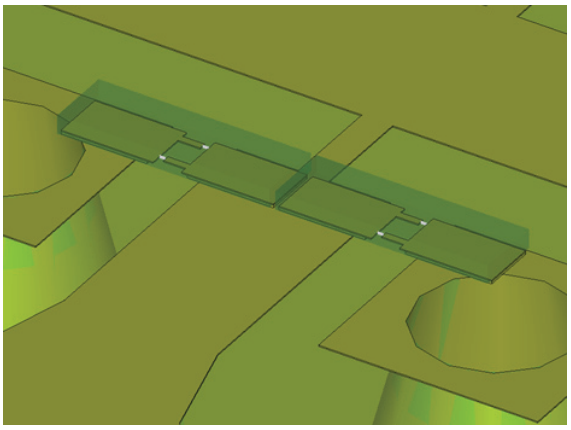

Figure 8 3D Model of two Anti-parallel Schottky Varistor diodes with internal ports (white) at each diode junction.

The six port s-parameter file was brought into AWR Microwave Office Harmonic Balance circuit simulator[12] with SPICE diode models attached to each internal port. The following is a list of SPICE Schottky Barrier Diode Varistor model[13] parameters used: RS = 10Ω, Is = 1e-11 A, N = 1.1, EG = 0.69, XTI = 2, CJO = 2.5 fF, BV = 5 V.

6 WR15 and WR5 Waveguide Transitions

To facilitate testing, two low loss, broadband WR15 and WR5 longitudinal E-Plane Waveguide-to-Microstrip transitions[14] were designed as a means to couple signals into and out from the planar Microstrip Tripler substrates as shown in Figure 9. For the longitudinal E-Plane probe transition designs, the microstrip enters the waveguide through a narrow slit in the waveguide's broad-wall. The substrate is oriented so its broad surface is orthogonal to the waveguides H-Field. With respect to the plane at the broad-wall window, a small series inductive transmission line is all that is needed to resonate out the capacitive reactance for the best broadband match. The WR-5 substrate probe width was required to be narrower, and thus a separate piece, from the integrated filter-diode-WR15-probe-transition substrate. This minimized the WR5 broad-wall aperture size and kept the next higher order mode above 220 GHz.

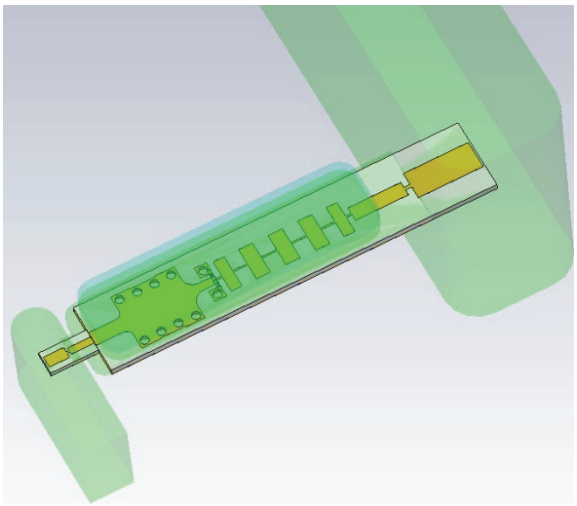

Figure 9 Complete 3D Electromagnetic model of G-Band Tripler.

Longitudinal E-Plane Waveguide-to-Microstrip transitions lend themselves to split block housing construction where the split plane of the housing is in the center of the waveguides broad-wall. The housing's back-short incorporates radii corresponding to the end mill tool radius used to machine the WR5 channel. The end mill tool radius used was one-half the narrow wall length. Incorporating back-short radii of one-half the narrow wall length increases the back-short distance 22% with respect to the substrate probe centerline from non-radii corners.

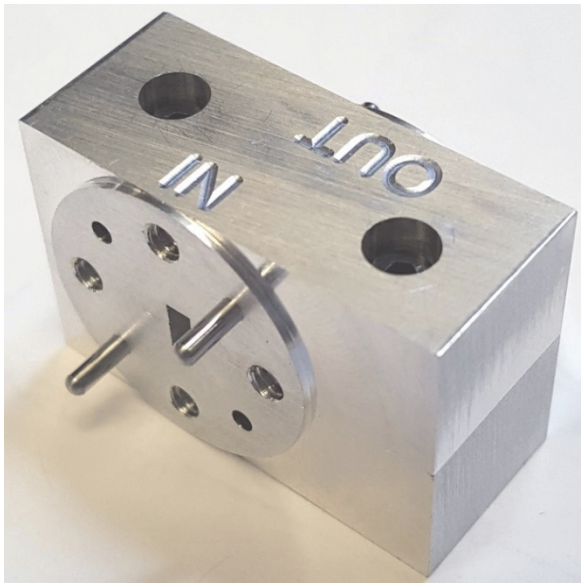

Figure 10 WR15-WR5 G-Band Tripler assembly.

7 Measurements

The setup shown in Figure 11 was used to test maximum power of two WR15 – WR5 flanged tripler assemblies shown in Figure 10. Figure 12 shows a plot of the measured maximum power frequency response. The simulated response in Figure 12 is the 3rd harmonic power component compressed by about 1-dB with a +10 dBm drive input. At the Tripler's WR15 port, the input power level where the Tripler compresses by 1-dB corresponds to a power range of +10 to +15 dBm. This measurement does capture all harmonic power at the Tripler's output but it is assumed the 5th harmonic is at least 10 dB below the desired 3rd harmonic due to relative conversion efficiency and losses. At compression, both tripler assemblies output power frequency response tracks each other well and varies only ±1.5 dB over the entire G-Band (140 GHz to 220 GHz).

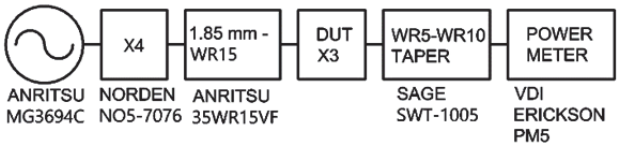

Figure 11 Block Diagram for testing WR15-WR5 G-Band Tripler maximum output power.

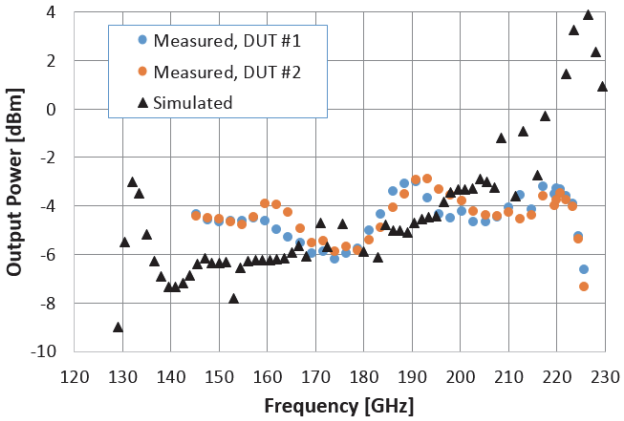

Figure 12 Measured and simulated maximum power frequency response of WR15-WR5 G-Band Tripler.

To examine the Tripler's 2nd and 3rd harmonic spectral content, a WR5 harmonic mixer was used at the Tripler's output to down-convert the tones shown in Figure 13. The frequency response of the 2nd harmonic shown in Figure 14 was measured with the 3rd harmonic output compressed by 1-dB. It was found this input power condition produced the worst case 2nd harmonic relative power level (to the desired 3rd harmonic). Rs and Cjo of one anti-parallel diode pair was varied 20% from nominal value to examine the effects of diode unbalance. For reference, the 2nd harmonic response with no diode parameter variation is included. Due to the high conversion loss of the harmonic mixer, harmonic levels below −50 dBc are not measureable on the spectrum

analyzer. Figure 15 shows a comparison of the 3rd harmonic response measured with a power meter and a harmonic mixer. This result shows the higher odd harmonics are well below the desired 3rd harmonic and has little influence on the power meter measurement.

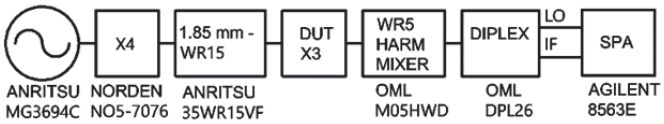

Figure 13 Block Diagram for testing output harmonics of WR15-WR5 G-Band Tripler.

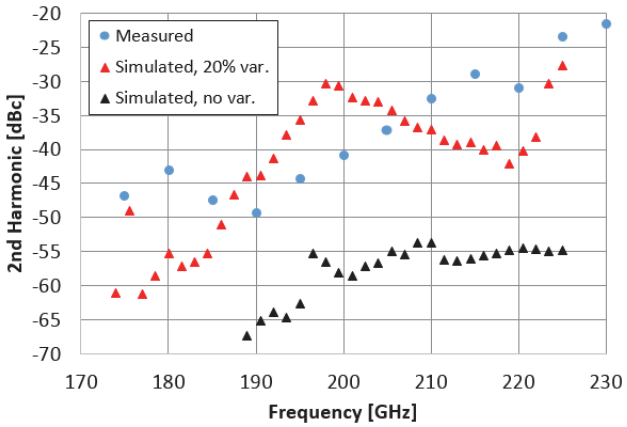

Figure 14 Measured and Simulated 2nd harmonic frequency response of WR15-WR5 G-Band Tripler at maximum 3rd harmonic power.

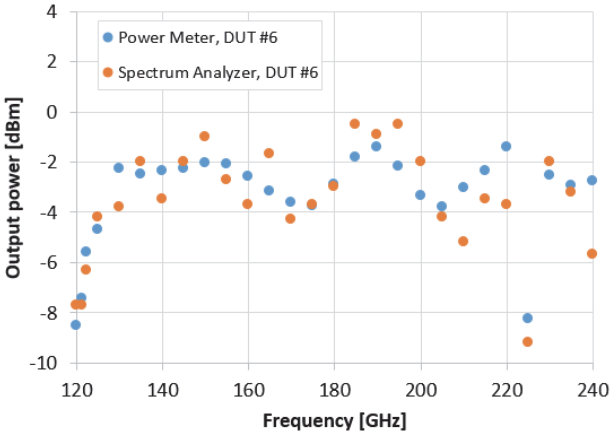

Figure 15 Measured and maximum power of WR15-WR5 G-Band Tripler using Power Meter and Spectrum Analyzer.

Beyond an input frequency of 73 GHz, the Norden N05-7076 quadrupler (×4) has sufficient output drive up to about 86 GHz to compress the tripler assembly. Up to 260 GHz, the maximum output power of the 3rd harmonic was measured to 265 GHz using the power measurement setup shown in Figure 11. With the exception of a few power drops at 226 GHz and 253 GHz, the maximum power does not vary more than ±4 dB up to 260 GHz as shown in Figure 16. It is likely the drops at 226 GHz and 253 GHz are due to higher modes produced by either the 35WR15VF adapter, WR15-microstrip transition or the WR5-microstrip band transition. These are band limited adapters and transitions so moding is expected operating outside their band. Higher order modes could also explain the simulation result peak at 225 GHz. The drop in power beyond 260 GHz is likely due to the passband roll-off of the 80 GHz LPF at the Tripler's input.

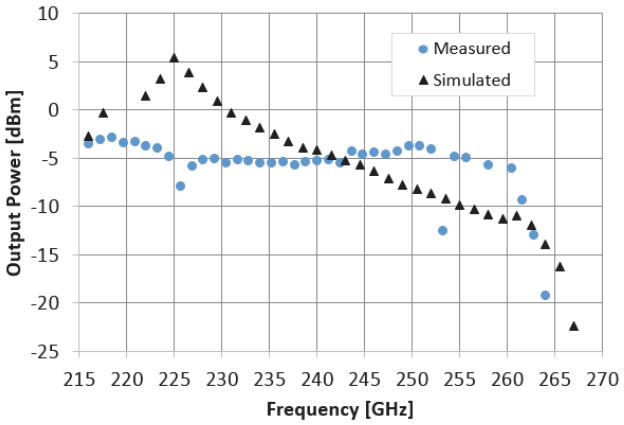

Figure 16 Measured and simulated maximum power of WR15-WR5 G-Band Tripler over an extended frequency.

8 Conclusions

We have successfully constructed and evaluated a G-Band Tripler with bandwidth that covers then entire 140 GHz to 220 GHz frequency range. The measurements show a maximum power of approximately −4 dBm with ±1.5 dB variation with +15 dBm input drive. The 2nd harmonic is greater than 29 dBc (referred to 3rd harmonic up to 220 GHz). Considering the band limited adapters and transitions present which allow testing of the tripler using standard waveguide and coaxial interfaces, the tripler element consisting of the input LPF, anti-parallel diodes and output HPF is shown to have an octave bandwidth that extends from 130 GHz to up to 260 GHz.

Acknolegement

The authors would like to thank the following Anritsu groups for providing their assistance with this project: Mechanical design staff for translating the 3D CAD models and designing the split block housing. Machining Center (MC)

for machining the split block housing, Microwave Technology Center (MTC) for fabricating the fused quartz substrates, and component assemebly staff for carefully putting these assembies together.

References

1) K. M. Noujeim, J. Martens, and T. Roberts, "Frequency-scalable nonlinear-transmission-line-based vector network analyzers," ARMMS 2011 Conference, Milton Mill House, Steventon, Oxfordshire, UK, April 5-6, 2011.
2) K. M. Noujeim, J. Martens, and T. Roberts, "A frequency-scalable NLTL-based signal-source extension," EuMC 2011, Manchester, UK, October 9-14, 2011.
3) J. Martens, T. Roberts, K. M. Noujeim, and S. Reyes, "70 KHz-145 GHz broadband S-parameter measurements: Calibration and verificationpossibilities", Proc. of the Asia Pacific Micr. Conf., Dec. 4-7, 2012, pp. 433-435.
4) M.J.W. Rodwell et al., "GaAs nonlinear transmission lines for picosecond pulse generation and millimeter-wave sampling," IEEE Trans. on Microwave Theory and Tech., vol. MTT-39, pp. 1194-1204, July 1991.
5) M. Hrobak, Critical mm-Wave Components for Synthetic Automatic Test Systems, Berlin, Germany, Springer Vieweg, 2015.
6) Porterfield D W. "High efficiency terahertz frequency tripler", IEEE MTT-S International Microwave Symposium, Honolulu, Hawaii, 2007: 337.
7) M. T. Faber, J. Chramiec, and M. E. Adamski, Microwave and millimeter-wave diode frequency multipliers, Artech House, Norwood, Mass., 1995.
8) Sonnet Software, Version 12.54, 126 N. Salina St., Syracuse, NY 1320.2, www.sonnetsoftware.com.
9) CST Microwave Studio, Version 2017, Bad Nauheimer Str. 19, 64289 Darmstadt, Germany, www.cst.com.
10) D. Deslandes, and K. Wu, "Integrated microstrip and rectangular waveguide in planar form", IEEE Microwave Wireless Components Letters, vol. 11, no. 2, Feb 2001, pp. 68-70.
11) F. Xu, and K. Wu, "Guided-Wave and leakage characteristics of substrate integrated waveguide," IEEE Trans. Microwave Theory Tech., vol. 53, no. 1, pp. 66–73, Jan. 2005.
12) AWR Microwave Office, National Instruments, E. Grand Ave., Suite 430, El Segundo, CA 90245, www.awrcorp.com.
13) P. Antognetti and G. Massobrio, "Semiconductor Device Modeling with SPICE", McGraw Hill, 2nd Ed. 1987.
14) Y. Leong, and S. Weinreb, "Full Band Waveguide-to-Microstrip Probe Transitions", IEEE International Microwave Symposium Digest, 1999, pp. 1435-1438.

Authors

Tom Roberts
Service Infrastructure Solutions
US Division
Measurement Business Division

Jon Martens
Service Infrastructure Solutions
US Division
Measurement Business Division

Publicly available